DOI: 10.1002/chem.201000679

The Equilibrium Between the Octahedral and Square Pyramidal Form and the Influence of an Axial Ligand on the Molecular Properties of $V^{IV}O$ Complexes: A Spectroscopic and DFT Study

Serge Gorelsky,[b] Giovanni Micera,[a] and Eugenio Garribba*[a]

Abstract: The previously unreported equilibrium in aqueous solution between the $V^{IV}O$ square pyramidal and *trans* octahedral form with an axial water molecule for a number of bidentate ligands with (N,O) and (O,O) donor sets (6-methylpicolinic (6-mepicH) and 6-methyl-2,3-pyridinedicarboxylic (6-me-2,3-pdcH_2) acids, dipyridin-2-ylmethanol (Hdpmo) and 1,2-dimethyl-3-hydroxy-4(1*H*)-pyridinone (Hdhp)) has been demonstrated by the combined application of EPR spectroscopy and DFT methods. The EPR spectra suggest that, with increasing ionic strength, the equilibrium is shifted towards the formation of the pentacoordinated species and values of $K \approx 4.0$ and 7.0 for the systems containing 6-methyl-2,3-pyridinedicarboxylic acid and dipyridin-2-ylmethanol were measured. DFT calculations performed with Gaussian 03 and ORCA software predict the ^{51}V anisotropic hyperfine coupling constant along the z axis (A_z), which can be used to demonstrate the presence of an axially bound ligand *trans* to the V=O bond. The results suggest that an axial donor (charged or not) can lower $|A_z|$, in contrast to what was previously believed on the basis of the "additivity rule", and this explains the anomalous behaviour of the $V^{IV}O$ complexes formed by *N*-{2-[(2-pyridylmethylene)amino]phenyl}-pyridine-2-carboxamide (Hcapca) and several amidrazone derivatives. The decrease in $|A_z|$ for the axial binding of a solvent molecule is mainly a result of the reduction of $|A_{iso}|$ and this was also observed when the solid [VO(6-methylpicolinato)$_2$] was dissolved in DMSO or DMF. The variations in the structural (V=O, V−O and V−N distances, O−V−O and N−V−N angles, and the trigonality index τ) and spectroscopic ($|A_z|$, $|A_{iso}|$ and ν(V=O)) properties as a function of the axial V−OH_2 distance (R) are also presented. Finally, the electronic structures of the penta- and hexacoordinated complexes are discussed.

Keywords: coordination modes · density functional calculations · electronic structure · EPR spectroscopy · vanadium

Introduction

Vanadium plays a number of roles in biological systems.[1] In particular, it is present in two enzymes, vanadium-dependent haloperoxidases[2] and nitrogenase.[3] In human organisms, it elicits a number of physiological responses, for example, the inhibition of phosphate-metabolising enzymes[4] such as phosphatases, ribonuclease and ATPases, and its compounds show insulin-enhancing activity.[5]

It has been suggested that, almost independently of the initial oxidation state, vanadium is transported in the blood as the $V^{IV}O$ form.[6–8] The geometry adopted in aqueous solution is often important for its biochemical functions: for example, the well-known insulin-enhancing compound [VO(mal)$_2$] (mal is maltolate) is square pyramidal in the solid state[9] and *cis* octahedral in solution with the two anionic ligands in an equatorial–equatorial and equatorial–axial arrangement and a water molecule in the fourth equatorial site.[10] Orvig and co-workers proposed that this structure should allow a histidine nitrogen atom of human serum albumin (HSA) to replace water in the equatorial plane thereby forming the *cis*-[VO(mal)$_2$(HSA)] adduct, which could be involved in transporting the drug to target sites in the human body and could be the pharmacologically active spe-

[a] Prof. G. Micera, Dr. E. Garribba
Dipartimento di Chimica and Centro Interdisciplinare
per lo Sviluppo della Ricerca Biotecnologica e
per lo Studio della Biodiversità della Sardegna
Università di Sassari, Via Vienna 2, I-07100 Sassari (Italy)
Fax: (+39) 079-229559
E-mail: garribba@uniss.it

[b] Dr. S. Gorelsky
Centre for Catalysis Research and Innovation
Department of Chemistry, University of Ottawa
10 Marie Curie Street BSC 431
K1N 6N5ON Ottawa, Ontario (Canada)

Supporting information for this article is available on the WWW under http://dx.doi.org/10.1002/chem.201000679.

cies.[11] Analogous results have recently been published by us for the biotransformation in blood serum of the potent insulin-enhancing agent $[VO(dhp)_2]$[12] (dhpH is 1,2-dimethyl-3-hydroxy-4(1*H*)-pyridinone), square pyramidal in the solid state but present as an equilibrium mixture of the pentacoordinated and *cis* octahedral forms in aqueous solution, to *cis*-$[VO(dhp)_2(HSA)]$ and *cis*-$[VO(dhp)_2(hTf)]$ mixed species (hTf is human serum apo-transferrin) after equatorial coordination of an imidazole nitrogen belonging to a surface histidine residue.[13]

Therefore it is very important for a chemist to have a tool to characterise the structure of $V^{IV}O$ species and establish which donors are coordinated to the metal ion. Electron paramagnetic resonance (EPR) spectroscopy has been shown to be the most powerful spectroscopic technique for investigating the electronic structure and geometry of a $V^{IV}O$ complex.[14] In fact, the identification of the equatorial donors of a $V^{IV}O$ species is possible by the application of the "additivity rule", first proposed by Wüthrich,[15] subsequently developed by Chasteen[16] and further improved by Pecoraro and co-workers.[17] It affirms that values of the ^{51}V anisotropic hyperfine coupling constants along the z axis (A_z) measured on a polycrystalline powder or a frozen sample can be calculated from the sum of the contributions of each equatorial donor function. Additions or corrections to the contribution of specific groups to expected A_z values ($|A_z|^{expct}$) have appeared in recent years in the literature.[18]

The "additivity rule" assumes that an axial ligand does not contribute to A_z so that its presence cannot be demonstrated by EPR spectroscopy. Therefore the possibility of the formation of an equilibrium between the $V^{IV}O$ species with and without a solvent (or ligand) molecule in the sixth coordination position (Scheme 1a and b) usually is not

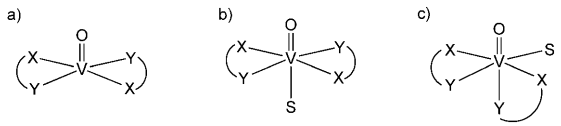

Scheme 1. a) Pentacoordinated square pyramidal, b) hexacoordinated *trans* octahedral and c) hexacoordinated *cis* octahedral forms of a bis-chelated $V^{IV}O$ complex. S is a solvent molecule.

taken into account. Few exceptions to the "additivity rule" have been reported in the literature: the octahedral complexes [VOX(capca)] (Hcapca is *N*-{2-[(2-pyridylmethylene)amino]phenyl}pyridine-2-carboxamide and X is an axial anion such as Cl^-, NCS^- or CH_3COO^-),[19] the solid species formed by eight amidrazone derivatives when they are dissolved in DMF[20] and two insulin-enhancing agents,[21] the bis-chelated complexes formed by 6-methylpicolinic and 6-ethylpicolinic acids.[22,23] In all cases a reduction of 10–15% with respect to the A_z value expected on the basis of the "additivity rule" is observed.

Whereas picolinate in aqueous solution stabilises only the *cis* arrangement,[24] the bis-chelated complex of 6-methylpicolinate $[VOL_2]$ is present as two species in equilibrium, considered until now to be the square-pyramidal and *cis* octahedral forms (Scheme 1a and c).[22] However, the characterisation of the supposed pentacoordinated species remains doubtful mainly because of the low $|A_z|$ value of the square-pyramidal complex ($149\times10^{-4}\,cm^{-1}$ compared with $165.6\times10^{-4}\,cm^{-1}$ predicted with the "additivity rule") and because the *cis* complex should be characterised by a pK_a value for the deprotonation of the equatorial water significantly lower than that of bulk water and give a mononuclear *cis*-hydroxo species $[VOL_2(OH)]^-$ with a $|A_z|$ value lower than that of $[VOL_2]$. However, none of these variations is observed. Thus, a reinterpretation of the results must be based on these considerations, which suggest that the *cis* isomer does not exist in aqueous solution.

For the moment, no convincing explanation of this phenomenon has appeared in the literature. Tolis et al. assumed that negatively charged ligands can induce the radial expansion of the singly occupied d_{xy} orbital thereby reducing the dipolar interaction ($P=g_e g_N \beta_e \beta_N \langle r^{-3}\rangle$) between the vanadium nucleus and the unpaired electron.[19b] We believe that this is only a partial analysis of the effect because it does not explain the reduction of $|A_z|$ for the bis complexes of 6-methylpicolinic and amidrazones (no charged ligands in the axial position) and the normal behaviour of *cis*-$[VO(pic)_2(H_2O)]$ (picH is picolinic acid) and its derivatives, for example, 5-(methoxycarbonyl)pyridine-2-carboxylic and 5-(isopropyloxycarbonyl)-2-pyridinecarboxylic acid (an axial carboxylate group).[24,25] Subsequently, Aznar et al. observed that a charged axial ligand reduces the electric field gradient along the V=O bond thereby decreasing the magnitude of the ^{51}V nuclear quadrupolar coupling constant (C_Q) and of $|A_z|$.[26]

In this work we re-examined this topic through the combined application of EPR spectroscopy and density functional theory (DFT) methods and tried to explain the incongruence between the experimental values and the predictions of the "additivity rule", throwing new light on the interpretation of the EPR results for $V^{IV}O$ complexes. We studied the behaviour in aqueous solution of the bis-chelated complexes formed by 6-methylpicolinic (6-mepicH) and 6-methyl-2,3-pyridinedicarboxylic (6-me-2,3-pdcH_2) acids, dipyridin-2-ylmethanol (Hdpmo) and 1,2-dimethyl-3-hydroxy-4(1*H*)-pyridinone (Hdhp) and in organic solvents of the solid species $[VO(6\text{-mepic})_2]$. Moreover, the complexes formed by Hcapca and one representative amidrazone derivative, N^1-(4-chlorobenzoyl)acetamidrazone (4-ClBzAmd), were reconsidered. The ligands discussed in the text are shown in Scheme 2 with the corresponding abbreviations. The main goals of the manuscript are 1) to discuss the previously unreported equilibrium between the octahedral and square-pyramidal forms, which may provide a new perspective on the interpretation of the EPR spectra of $V^{IV}O$ sites contained in simple coordination compounds, biomolecules and metalloproteins, 2) to show the influence of an axial ligand on structural (V=O and equatorial V–L distances, L–V–L angles and the trigonality index τ) and spectroscopic (^{51}V hyperfine coupling constants $|A_z|$ and $|A_{iso}|$ and the

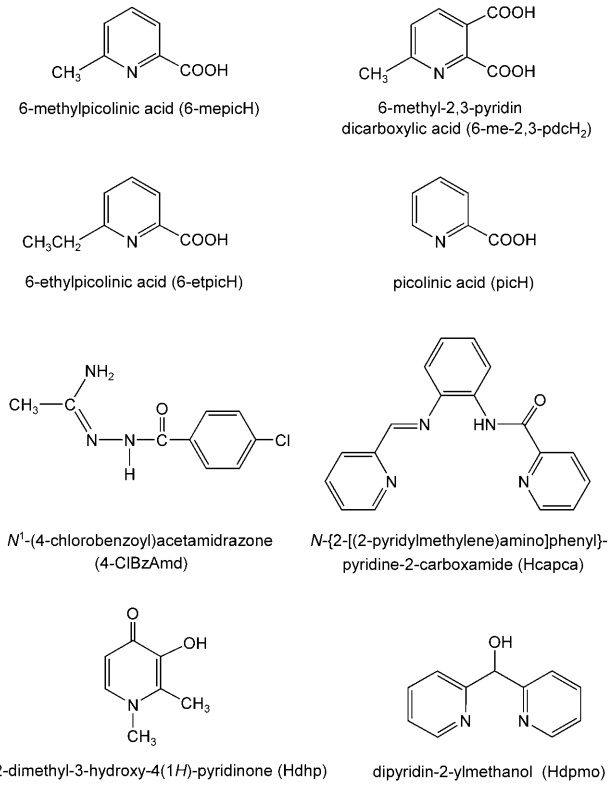

Scheme 2. Ligands and their abbreviations.

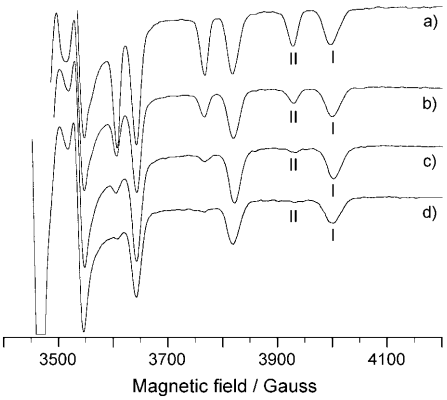

Figure 1. X-band anisotropic EPR spectra (120 K) of the $V^{IV}O$/6-me-2,3-pdcH_2 system recorded at pH 5.5 as a function of ionic strength I ($NaClO_4$) at a $V^{IV}O$ concentration of 4 mM and a molar ratio of 1:2. a) 0.016 M, b) 0.040 M, c) 0.250 M and d) 2.000 M. **I** and **II** indicate the resonances of $[VO(6\text{-me-}2,3\text{-pdc})_2]^{2-}$ and *trans*-$[VO(6\text{-me-}2,3\text{-pdc})_2(H_2O)]^{2-}$, respectively.

stretching frequency of the V=O bond ν(V=O) properties, 3) to present the theoretical basis for these effects and 4) to highlight the performance of DFT methods in the characterisation of such systems. The results could have implications in the study of the interactions between vanadium and biomolecules.

Results and Discussion

Behaviour in water and in organic solvents: The behaviour in aqueous solution of the bis-chelated complexes formed by 6-methylpicolinic and 6-methyl-2,3-pyridinedicarboxylic acids has been examined as a function of the ionic strength (I), varied by the addition of $NaClO_4$. Preliminary pH-metric studies on the aqueous $V^{IV}O$/6-me-2,3-pdcH_2 system suggest that at pH > 4 all the carboxylic groups are deprotonated and the species $[VO(6\text{-me-}2,3\text{-pdc})_2]^{2-}$ is formed. This is in agreement with what was observed for 6-methylpicolinate, which in water between pH 4 and 6 is present as $[VO(6\text{-mepic})_2]$.[22] 6-Methyl-2,3-pyridinedicarboxylate has the advantage that it forms a soluble dianionic bis-chelated complex rather than a solid species.

Anisotropic EPR spectra recorded for the $V^{IV}O$/6-me-2,3-pdcH_2 system are presented in Figure 1. They consist of two sets of spectral resonances, the outer with $|A_z| = 160 \times 10^{-4}\,cm^{-1}$ (**I** in Figure 1) and the inner with $|A_z| = 147 \times 10^{-4}\,cm^{-1}$ (**II** in Figure 1); the surprising observation is that, with increasing ionic strength, the inner signals disappear and the outer increase in intensity. Because species **I** and **II** are characterised by the same stoichiometric composition ($[VOL_2]^{2-}$ if the ligand in its fully protonated form is indicated as LH_2), these results can be simply explained by postulating an equilibrium between the pentacoordinated square pyramid (species **I**) and the hexacoordinated octahedral form with a water molecule in the axial position (species **II**), represented in Scheme 3.

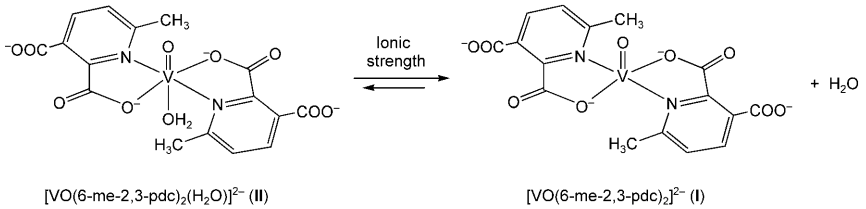

Scheme 3. Equilibrium between the octahedral and square pyramidal bis-chelated $V^{IV}O$ complexes of 6-methyl-2,3-pyridinedicarboxylate.

Similar behaviour has been demonstrated for tetra-aza Ni^{II} complexes, for example, those formed by triethylenetriamine (trien), which in water exist as an equilibrium mixture of a paramagnetic octahedral and a diamagnetic square-planar form.[27]

The tendency of this class of ligands (the derivatives of 6-methylpicolinic acid) to coordinate an axial water *trans* to the V=O group, in contrast to acetylacetonate and maltolate, for example,[9,28] is interestingly confirmed by the solid

species formed by 6-ethylpicolinic (6-etpicH) and 2-quinolinecarboxylic acids, the X-ray structures of which have been reported in the literature: both are octahedral with a water molecule axially coordinated at around 2.3 Å.[23,29] No particular solid-state effects, which may force the coordination of the solvent molecule in the sixth coordination position (these compounds precipitate from water or a water/ethanol mixture, respectively) seem to be operating.

The spectroscopic observations can be explained in this way: with increasing ionic strength, the activity coefficients (f) of the two anionic complexes decrease in a comparable way, whereas the lowering of the activity coefficient of water is not compensated and the equilibrium shifts towards the right [Eq. (1)].[27]

$$K = \frac{[\mathrm{VO(6\text{-}me\text{-}2,3\text{-}pdc)_2}]^{2-} f_{[\mathrm{VO(6\text{-}me\text{-}2,3\text{-}pdc)_2}]^{2-}} [\mathrm{H_2O}] f_{\mathrm{H_2O}}}{[\mathrm{VO(6\text{-}me\text{-}2,3\text{-}pdc)_2(H_2O)}]^{2-} f_{[\mathrm{VO(6\text{-}me\text{-}2,3\text{-}pdc)_2(H_2O)}]^{2-}}} = K_c \frac{f_{[\mathrm{VO(6\text{-}me\text{-}2,3\text{-}pdc)_2}]^{2-}} f_{\mathrm{H_2O}}}{f_{[\mathrm{VO(6\text{-}me\text{-}2,3\text{-}pdc)_2(H_2O)}]^{2-}}} \quad (1)$$

For each value of the ionic strength, K_c can be calculated from Equation (2) in which $M_{I,-7/2}$(sp) and $M_{I,-7/2}$(o) are the EPR intensities corresponding to the first parallel transition of the square-pyramidal and *trans* octahedral species. The areas subtended by such resonances can be measured very well because the spectral lines do not superimpose in the low-field region. The extrapolation at $I=0$ yields $K=4.0\pm 0.7$; this value suggests that at low ionic strength the pentacoordinated form is slightly favoured. It must be pointed out that, since the intensity of the EPR signal of the octahedral species is very low with respect to that of the square-pyramidal complex for an ionic strength greater than 0.25 M (see Figure 1), the values of K_c are affected by an uncertainty that, increases with I; this explains the rather large error in the value of the equilibrium constant K. However, we would stress that the exact determination of K is beyond the goals of this work in which we have focused our attention on the qualitative analysis of the equilibrium between the two $V^{IV}O$ species. The results are displayed in Figure 2.

$$K_c = \frac{M_{I,-7/2}(\mathrm{sp})}{M_{I,-7/2}(\mathrm{o})} \quad (2)$$

For 6-methylpicolinate only qualitative measurements are possible due to the presence of the solid complex [VO(6-mepic)$_2$] in the concentration range used.[22]

The new interpretation of the experimental data also explains (Figure 3) 1) the coincidence of $|A_z|$ of the square-pyramidal species **I** with that of analogous complexes provided by the 2(N_{pyr}, COO^-) donor set, like those formed by 2-pyridineacetic and 1-isoquinolinecarboxylic acids (161×10^{-4} cm^{-1}), which some of us are currently studying,[30] and 2) the difference between the $|A_z|$ values for the square-pyramidal species **I** and the *cis* species formed by picolinic acid and its derivatives ($\sim$165–168$\times 10^{-4}$ cm^{-1})[24,25] in which the *cis* arrangement of the two ligand molecules has been unambiguously demonstrated by X-ray diffraction analysis.[25]

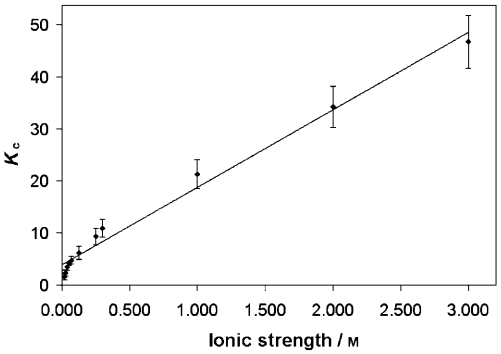

Figure 2. Values of K_c, calculated as the ratio of the EPR intensities corresponding to the first parallel transition ($M_I=-7/2$) of the square-pyramidal [VO(6-me-2,3-pdc)$_2$]$^{2-}$ ($M_{I,-7/2}$ (sp)) and octahedral *trans*-[VO(6-me-2,3-pdc)$_2$(H$_2$O)]$^{2-}$ species ($M_{I,-7/2}$ (o)), plotted as a function of ionic strength I ($NaClO_4$). The $V^{IV}O$ concentration was 4 mM and the molar ratio 1:2. The spectra were recorded at 120 K.

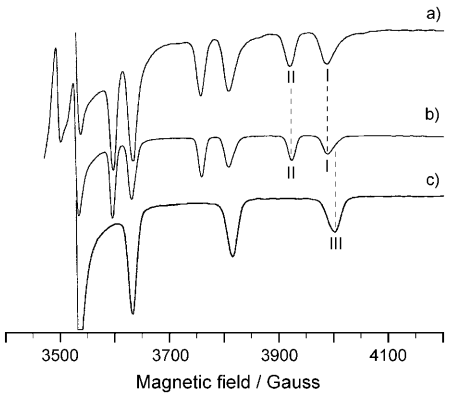

Figure 3. High-field region of the X-band anisotropic EPR spectra (120 K) recorded in aqueous solution for the systems $V^{IV}O$/L with a $V^{IV}O$ concentration of 4 mM and molar ratio of 1:2. a) L = 6-me-2,3-pdcH$_2$, b) L = 6-mepicH and c) L = picH. **I** and **II** indicate the resonances of [VOL_2]$^{x-}$ and *trans*-[$VOL_2(H_2O)$]$^{x-}$ ($x=2$ for 6-me-2,3-pdcH$_2$ and $x=0$ for 6-mepicH) and **III** indicates the resonances of *cis*-[$VOL_2(H_2O)$].

The behaviour of the solid [VO(6-mepic)$_2$] complex after dissolution in DMSO and DMF gives further insights (Figure 4); it precipitates in the square-pyramidal form without water molecules coordinated to the metal ion.[21,22,31] When it is dissolved in DMSO, the results are similar to those obtained in water with a mixture of *trans*-[VO(6-mepic)$_2$(dmso)] and [VO(6-mepic)$_2$] being detected; analogous findings have been observed with the structurally similar ligand, 6-ethylpicolinate.[23] In DMF, however, only one species is revealed and the $|A_z|$ value suggests that it is the octahedral species with an axial solvent molecule; this indicates that axial binding is preferred in DMF rather than in DMSO. Moreover, the experimental $|A_z|$ values for the octahedral species (149 cm^{-1} in DMF and 150×10^{-4} cm^{-1} in DMSO), similar to those measured for *trans*-[VO(6-mepic)(H$_2$O)], suggest that a water, a DMSO or a DMF molecule

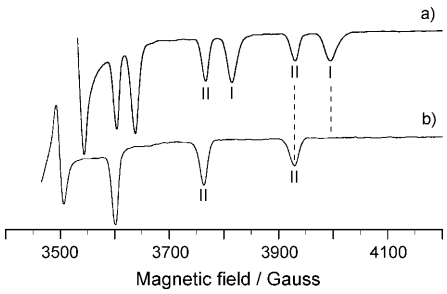

Figure 4. High-field region of the X-band anisotropic EPR spectra (120 K) of the solid *trans*-[VO(6-mepic)$_2$] complex dissolved in a) DMSO and b) DMF. **I** indicates the resonances of *trans*-[VO(6-mepic)$_2$] and **II** the resonances of *trans*-[VO(6-mepic)$_2$(dmso)] (trace a) or *trans*-[VO(6-mepic)$_2$(dmf)] (trace b).

axially bound to $V^{IV}O$ ion should have a similar effect on the EPR parameters and lower the ^{51}V hyperfine coupling constant along the z axis by a comparable amount.

After these observations for the 6-methylpicolinic and 6-methyl-2,3-pyridinedicarboxylic acids, we wondered whether this type of behaviour for $V^{IV}O$ complexes could be more frequent than what is currently believed. Very recently, we proposed the same explanation for the species with stoichiometry [VO(dpmoH$_{-1}$)$_2$] formed by dipyridin-2-ylmethanol in the pH range 5–10 with a ligand-to-metal molar ratio of 2.[32] The square-pyramidal and *trans* octahedral species are characterised by $|A_z|$ values of 151×10^{-4} and 144×10^{-4} cm^{-1}, respectively.[32] Whereas the $|A_z|$ value for [VO(dpmoH$_{-1}$)$_2$] is comparable to that expected on the basis of the "additivity rule" ($|A_z|^{expct}\sim152\times10^{-4}$ cm^{-1} for the coordination mode 2(N$_{pyr}$, O$^-$)), that for *trans*-[VO(dpmoH$_{-1}$)$_2$(H$_2$O)] is sensibly lower. In this work the EPR spectra of the $V^{IV}O$/Hdpmo (1:2) system at pH 7, at which the bis-chelated species reaches its maximum extent formation, were recorded as a function of ionic strength ($NaClO_4$) and are shown in Figure S10 of the Supporting Information.

From an examination of Figure S10, behaviour very similar to that for the 6-methyl-2,3-pyridinedicarboxylic acid system can be observed and the equilibrium constant obtained, $K=7.0\pm0.3$, suggests that for dipyridin-2-ylmethanol the formation of the square-pyramidal species is favoured. The values of K_c, calculated by the same procedure used for the system with 6-methyl-2,3-dicarboxylate, are plotted as a function of ionic strength (I) in Figure S11 of the Supporting Information.

Finally, the EPR spectra recorded during a study of the biotransformation of [VO(dhp)$_2$] in blood serum[13] reveal the presence of an additional species besides the well-known square-pyramidal [VO(dhp)$_2$] and the *cis* octahedral *cis*-[VO(dhp)$_2$(H$_2$O)] (Figure S12 of the Supporting Information). We attributed these previously unreported weak resonances to *trans*-[VO(dhp)$_2$(H$_2$O)]; they can probably be detected in these experimental conditions because of the lower value of the ionic strength ($I=0.002$ M) with respect to that used in the previous studies ($I=0.008$ M).[33]

Note that the possibility of a *cis* and *trans* arrangement of the unsymmetrical bidentate ligands across the equatorial plane, which could in principle be realised, has not been taken into account. This assumption is supported by a recent search of the Cambridge Structural Database[34] for pentacoordinated [VOL$_2$] complexes formed by bidentate ligands (symmetrical and unsymmetrical): for all 59 structures found, the arrangement of the ligands across the equatorial plane is *trans*.[35]

Optimisation of the structures and calculation of EPR parameters by DFT methods: Here we try to prove the hypothesis presented above by DFT methods. They allow calculation of the EPR parameters of transition-metal complexes[36] and more particularly of $V^{IV}O$ species.[26,37] Recently we achieved consistent success in predicting the ^{51}V hyperfine coupling constants by using the Gaussian 03 software.[38] We calculated the A_z values of 22 representative $V^{IV}O$ complexes of different charge, geometry and coordination mode at the BHandHLYP/6-311g(d,p) level of theory with a mean deviation of 2.7% from the experimental values.[39] The results are particularly good in the case of neutral $V^{IV}O$ complexes with (N, O) donor ligands (mean deviation of 1.6% for the species studied in ref.[39]), like those considered in this work. The use of half-and-half hybrid functionals, which allows treatment of core–shell spin polarisation, seems to be necessary to obtain satisfactory agreement with experimental results.[37b,39] In this work we also performed simulations of the A_z values for the complexes studied with the ORCA software,[40] which on one hand does not allow for the use of half-and-half functionals but on the other considers the second-order spin–orbit contribution to the $\boldsymbol{A}$ tensor.[37c]

The structures of the complexes studied were optimised with Gaussian 03 at the B3LYP/6-311g(d) level of theory. The calculated structure of *trans*-[VO(6-mepic)$_2$(H$_2$O)] (Figure 5) shows good agreement with the experimental X-ray structure of *trans*-[VO(6-etpic)$_2$(H$_2$O)] (Table 1):[23] the absolute mean deviation is 1.9% for the bond lengths and 3.2% for the bond angles. Only the axial distance V–OH$_2$ (2.470 Å calculated vs. 2.283 Å experimental) significantly deviates from the experimental value, but it must be taken into account that the simulations were performed in the gas phase and the secondary hydrogen-bonding effects between

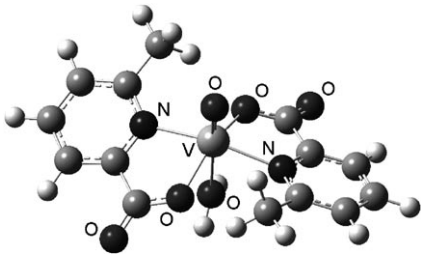

Figure 5. Optimised structure of *trans*-[VO(6-mepic)$_2$(H$_2$O)] at the B3LYP/6-311g(d) level of theory. The hydrogen atoms have been omitted for clarity.

Table 1. Structural details of $V^{IV}O$ complexes formed by 6-mepicH and 6-etpicH calculated at the B3LYP/6-311g(d) level of theory.[a]

Bond length/ angle	[VO(6-mepic)$_2$]	*trans*-[VO(6-mepic)$_2$(H_2O)]	*trans*-[VO(6-etpic)$_2$-(H_2O)][b]
V=O	1.573	1.572	1.571(4)
V–N	2.143	2.160	2.146(2), 2.153(3)
V–O	1.935	1.971	1.956(3), 2.001(8)
V–OH_2	–	2.470	2.283(2)
O=V-N	101.6	97.6	94.4(2), 97.1(7)
O=V-O	116.7	107.6	100.7(8), 102.3(7)
O=V-OH_2	–	180.0	176.9(8)
N-V-N	156.8	164.9	167.8(3)
O-V-O	126.5	144.9	156.7(2)
τ	0.505	0.333	0.185(2)

[a] All values are given in Å and in degrees. [b] X-ray structure reported in ref. [23].

the coordinated H_2O ligand and the solvent were not included in the calculations. However, the variation in the energy when the distance V–OH_2 (R) is in the range of 2.3–2.6 Å is not significant (see Figure 6) and therefore packing factors and solid-state effects may be important in determining the experimental value of R in the solid *trans*-[VO(6-etpic)$_2$(H_2O)]. For example, the water molecule is 2.385 Å from vanadium in the species *trans*-[VO{*N*,*N*′-bis(3-methoxysalicylidene)ethane-1,2-diaminato}(H_2O)].[41]

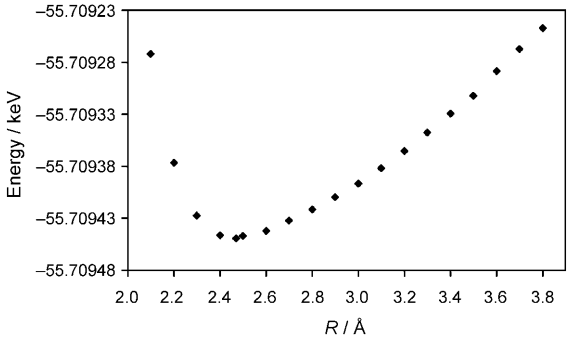

Figure 6. Variation of the energy of the *trans*-[VO(6-mepic)$_2$(H_2O)] complex as a function of the distance V–OH_2 (R).

A comparison between the calculated and experimental structures of 1) *cis*-[VO(pic)$_2$(H_2O)], *cis*-[VO{5-(methoxycarbonyl)pyridine-2-carboxylato}$_2$(H_2O)][26a] and *cis*-[VO{5-(isopropyloxycarbonyl)-2-pyridinecarboxylato}$_2$(H_2O)],[26b] 2) [VO(dpmoH_{-1})$_2$], [VO(2-mentholpyridineH_{-1})$_2$][42] and [VO{9-(2-pyridyl)fluoren-9-olato}$_2$]·0.5CH_2Cl_2,[43] and 3) [VO(dhp)$_2$] and [VO(mal)$_2$][9] confirms this agreement (Tables S3, S6 and S7 of the Supporting Information). For pentacoordinated $V^{IV}O$ species an important structural parameter is the trigonality index τ, which is a measure of the distortion of a square-pyramidal structure, in which the two equatorial L–V–L angles are 180°, towards a trigonal bipyramid, characterised by an angle of 180° (axial donors) and another of 120° (equatorial donors): τ is defined as $(\beta-\alpha)/60$, in which β and α are the angles formed by the two pseudoaxial and two pseudoequatorial donors, and is 1 and 0 for ideal trigonal-bipyramidal and square-pyramidal complexes, respectively.[44] An examination of the optimised structure of [VO(dpmoH_{-1})$_2$] and the experimental structures of [VO(2-mentholpyridineH_{-1})$_2$][42] and [VO{9-(2-pyridyl)fluoren-9-olato}$_2$]·0.5CH_2Cl_2[43] (Table S6 of the Supporting Information), characterised by identical 2(N_{pyr}, O^-) coordination, shows that the prediction of the N–V–N (β) and O–V–O (α) angles and τ is very good.

EPR parameters calculated with Gaussian 03 at the BHandHLYP/6-311g(d,p) level of theory are listed in Table 2. With the ORCA software, the Ahlrichs-VTZ basis set coupled to five different functionals (B3LYP, BP86, B3PW, TPSSh and PBE0) was used. The best results were obtained with PBE0, the one parameter hybrid version of

Table 2. ^{51}V hyperfine coupling constants of $V^{IV}O$ complexes calculated with the Gaussian 03 software, expected on the basis of the "additivity rule" (A^{expct}) and experimentally determined (A^{exptl}).[a]

Complex	$A^{FC}=A_{iso}$	A_x^D	A_y^D	A_z^D	A_x	A_y	A_z	A_z^{expct}[b]	A_z^{exptl}[c]	Dev. [%][d]
trans-[VO(6-mepic)$_2$(H_2O)]	−83.0	38.8	29.0	−67.8	−44.2	−54.0	−150.8	−165.6	−149.0[e]	+1.2
[VO(6-mepic)$_2$]	−90.4	38.5	30.1	−68.6	−51.9	−60.3	−159.0	−165.6	−160.8[f]	−1.1
trans-[VO(6-mepic)$_2$(dmf)]	−81.9	39.1	28.5	−67.6	−42.8	−53.4	−149.5	−165.6	−148.8[f]	+0.5
trans-[VO(6-mepic)$_2$(dmso)]	−82.2	39.1	28.6	−67.7	−43.1	−53.6	−149.9	−165.6	−148.6[f]	+0.9
trans-[VO(6-etpic)$_2$(dmso)]	−83.4	39.1	28.8	−67.9	−44.3	−54.6	−151.3	−165.6	−150.1[g]	+0.8
trans-[VO(6-me-2,3-pdc)$_2$(H_2O)]$^{2-}$	−81.5	38.9	28.5	−67.4	−42.6	−53.0	−148.9	−165.6	−146.5[f]	+1.6
[VO(6-me-2,3-pdc)$_2$]$^{2-}$	−89.5	38.4	29.9	−68.3	−51.1	−59.6	−157.8	−165.6	−160.1[f]	−1.4
cis-[VO(pic)$_2$(H_2O)]	−100.2	34.9	32.6	−67.5	−65.3	−67.6	−167.7	−169.1	−165.0[g]	+1.6
trans-[VO(4-ClBzAmd)$_2$(dmf)]$^{2+}$	−86.9	37.0	26.9	−63.9	−49.9	−60.0	−150.8	−170.2	−148.2[h]	+1.8
[VO(4-ClBzAmd)$_2$]$^{2+}$	−98.7	37.0	30.6	−67.6	−61.7	−68.1	−166.3	−170.2	[i]	
trans-[VOCl(capca)]	−84.6	40.6	23.1	−63.7	−44.0	−61.5	−148.3	−155.7	−145.0[j]	+2.3
trans-[VO(NCS)(capca)]	−83.8	39.8	23.7	−63.5	−44.0	−60.1	−147.3	−155.7	−148.0[j]	−0.5
[VO(capca)]$^+$	−90.6	38.3	29.0	−67.3	−52.3	−61.6	−157.9	−155.7	[i]	
trans-[VO(dpmoH_{-1})$_2$(H_2O)]	−77.4	38.1	29.6	−67.7	−39.3	−47.8	−145.1	−152.0	−143.8[k]	+0.9
[VO(dpmoH_{-1})$_2$]	−84.9	37.3	30.9	−68.2	−47.6	−54.0	−153.1	−152.0	−151.2[k]	+1.3
trans-[VO(dhp)$_2$(H_2O)]	−83.2	39.1	28.9	−68.0	−44.1	−54.3	−151.2	−164.8	−150.8[f]	+0.3
[VO(dhp)$_2$]	−90.3	39.1	30.1	−69.2	−51.2	−60.2	−159.5	−164.8	−157.4[l]	+1.3
cis-[VO(dhp)$_2$(H_2O)]	−101.1	35.5	33.2	−68.7	−65.6	−67.9	−169.8	−169.2	−166.0[l]	+2.3

[a] All values are given in 10^{-4} cm^{-1} units. [b] Value expected on the basis of the "additivity rule". [c] Experimental value. [d] Percent deviation from $|A_z|^{exptl}$ calculated from $100[(|A_z|^{calcd}-|A_z|^{exptl})/|A_z|^{exptl}]$. [e] Ref. [22]. [f] This work. [g] Ref. [23]. [h] Ref. [20]. [i] Not existing structure. [j] Ref. [19]. [k] Ref. [32]. [l] Ref. [33a].

Table 3. ^{51}V hyperfine coupling constants of $V^{IV}O$ complexes calculated with the ORCA software (A) and experimentally determined (A^{exptl}).[a]

Complex	A^{FC}	A_x^D	A_y^D	A_z^D	A_x^{SO}	A_y^{SO}	A_z^{SO}	A_{iso}	A_x	A_y	A_z	A_z^{exptl}[b]	Dev. [%][c]
trans-[VO(6-mepic)$_2$(H$_2$O)]	−71.9	37.9	26.3	−64.1	−2.9	−3.8	−9.0	−77.1	−36.9	−49.4	−145.0	−149.0[d]	−2.7
[VO(6-mepic)$_2$]	−79.5	37.1	27.8	−64.9	−2.7	−3.5	−9.2	−84.6	−45.1	−55.2	−153.6	−160.8[e]	−4.5
trans-[VO(6-mepic)$_2$(dmf)]	−71.6	38.1	26.0	−64.1	−2.9	−3.9	−9.0	−76.9	−36.4	−49.5	−144.7	−148.8[e]	−2.8
trans-[VO(6-mepic)$_2$(dmso)]	−71.7	38.1	26.0	−64.1	−2.9	−3.9	−9.0	−77.0	−36.5	−49.6	−144.8	−148.6[e]	−2.6
trans-[VO(6-etpic)$_2$(dmso)]	−73.1	38.0	26.2	−64.2	−2.9	−3.8	−9.0	−78.3	−38.0	−50.7	−146.3	−150.1[f]	−2.5
trans-[VO(6-me-2,3-pdc)$_2$(H$_2$O)]$^{2-}$	−71.0	38.0	26.0	−64.0	−2.9	−3.8	−9.0	−76.2	−35.9	−48.8	−144.0	−146.5[e]	−1.7
[VO(6-me-2,3-pdc)$_2$]$^{2-}$	−79.2	37.2	27.6	−64.8	−2.7	−3.4	−9.3	−84.3	−44.7	−55.0	−153.3	−160.1[e]	−4.2
cis-[VO(pic)$_2$(H$_2$O)]	−90.3	32.6	30.9	−63.5	−3.2	−3.3	−9.8	−95.7	−60.9	−62.7	−163.6	−165.0[d]	−0.8
trans-[VO(4-ClBzAmd)$_2$(dmf)]$^{2+}$	−73.2	36.7	24.9	−61.6	−2.9	−3.6	−9.6	−78.6	−39.4	−51.9	−144.4	−148.2[g]	−2.6
[VO(4-ClBzAmd)$_2$]$^{2+}$	−84.7	35.9	27.9	−63.8	−2.5	−3.1	−8.9	−89.5	−51.3	−59.9	−157.4	[h]	
trans-[VOCl(capca)]	−72.7	39.9	19.9	−59.8	−2.9	−3.8	−10.0	−78.3	−35.7	−56.6	−142.5	−145.0[i]	−1.7
trans-[VO(NCS)(capca)]	−73.1	39.2	20.8	−60.0	−3.0	−3.9	−9.8	−78.7	−36.9	−56.2	−142.9	−148.0[i]	−3.4
[VO(capca)]$^+$	−78.6	37.3	26.7	−64.0	−2.7	−3.4	−8.6	−83.5	−44.0	−55.3	−151.2	[h]	
trans-[VO(dpmoH$_{-1}$)$_2$(H$_2$O)]	−66.8	36.9	27.2	−64.1	−2.9	−3.9	−8.6	−71.9	−32.8	−43.5	−139.5	−143.8[j]	−3.0
[VO(dpmoH$_{-1}$)$_2$]	−74.0	35.5	28.7	−64.2	−2.8	−3.4	−8.8	−79.0	−41.3	−48.7	−147.0	−151.2[j]	−2.8
trans-[VO(dhp)$_2$(H$_2$O)]	−73.9	38.1	26.3	−64.4	−3.1	−4.3	−10.0	−79.7	−38.9	−51.9	−148.3	−150.8[e]	−1.7
[VO(dhp)$_2$]	−80.4	37.9	27.4	−65.3	−2.9	−3.9	−10.1	−86.0	−45.4	−56.9	−155.8	−157.4[k]	−1.0
cis-[VO(dhp)$_2$(H$_2$O)]	−92.7	33.8	31.1	−64.9	−3.4	−4.0	−10.9	−98.8	−62.3	−65.6	−168.5	−166.0[k]	+1.5

[a] All values are given in 10^{-4} cm^{-1} units. [b] Experimental value. [c] Percent deviation from $|A_z|^{exptl}$ calculated from $100[(|A_z|^{calcd}-|A_z|^{exptl})/|A_z|^{exptl}]$. [d] Ref. [22]. [e] This work. [f] Ref. [23]. [g] Ref. [20]. [h] Not existing structure. [i] Ref. [19]. [j] Ref. [32]. [k] Ref. [33a].

the Perdew–Burke–Erzerhoff GGA functional, and the calculated A_z values are reported in Table 3.

From a comparison of the data in Tables 2 and 3, it can be seen that the mean deviation from the experimental value of A_z ($|A_z|^{exptl}$) is 1.2% with Gaussian 03 and 2.5% with ORCA. Note that this latter value underestimates the values of $|A_z^{FC}|$ and $|A_z^{D}|$ with respect to Gaussian 03, but includes the term A_z^{SO}, which makes a contribution of about 6% to A_z^{calcd}. However, it is also important to note that the ORCA software can be used to satisfactorily predict A_z values for a $V^{IV}O$ species if a simulation at the PBE0/VTZ level of theory is performed and if the calculation of the spin–orbit contribution to $\boldsymbol{A}$ is included in the input file.

The data in Tables 2 and 3 reveal the following points.

1) DFT methods (either using the half-and-half functional with Gaussian 03 or considering the spin–orbit contribution to the hyperfine coupling constant with ORCA) predict a low $|A_z|$ value for all the octahedral species with a solvent or ligand molecule coordinated in the axial position and this explains the behaviour of the complexes formed by Hcapca[19] and by amidrazones.[20] The significant reduction in $|A_z|$ for the hexacoordinated form is mainly a result of the decrease in $|A_{iso}|$ rather than the $|A_z^{D}|$ or $|A_z^{SO}|$ term. These assumptions were proved by the isotropic EPR spectra of the $V^{IV}O$/6-mepicH and $V^{IV}O$/6-me-2,3-pdcH$_2$ systems recorded at room temperature, which show the same behaviour as the resonances of *trans*-[VO(6-mepic)$_2$(H$_2$O)] and *trans*-[VO(6-me-2,3-pdc)$_2$(H$_2$O)]$^{2-}$ found at low temperatures, decreasing in intensity with increasing ionic strength (Figure S13 of the Supporting Information). [VO(6-mepic)$_2$] and [VO(6-me-2,3-pdc)$_2$]$^{2-}$ are characterised by $|A_{iso}|$ values of 90.7 and 89.7×10^{-4} cm^{-1} and the corresponding *trans* octahedral species by values of 77.2 and 76.4×10^{-4} cm^{-1}. These values are very similar to those calculated by DFT methods with the Gaussian 03 and ORCA software (Tables 2 and 3).
2) A_z values calculated for the pentacoordinated square-pyramidal complexes (Scheme 1a) [VO(6-mepic)$_2$], [VO(6-me-2,3-pdc)$_2$]$^{2-}$, [VO(dpmoH$_{-1}$)$_2$] and [VO(dhp)$_2$] and for the *cis* structures (Scheme 1c) formed by picolinate and 1,2-dimethyl-3-hydroxy-4(1*H*)-pyridinonate are very similar to the experimental values. Thus, it can be stated that such structures do not constitute an exception to the "additivity rule".
3) "Normal" values, in agreement with those expected on the basis of the "additivity rule", are predicted for the two hypothetical square-pyramidal [VO(4-ClBzAmd)$_2$]$^{2+}$ and [VO(capca)]$^+$, which further demonstrates that it is the sixth axial ligand that causes the reduction of the $|A_z|$ value.

As a final comment, it should be highlighted that DFT methods appear to be a potent tool for predicting the A_z value of a $V^{IV}O$ species and those that seem to be exceptions are, as a matter of fact, normal behaviour not fully considered by the "additivity rule". Therefore the effect of an axial ligand, charged as in [VOX(capca)] or neutral as in the complexes discussed in this work, is intrinsically considered by DFT methods. One could ask why $|A_z|$ for *cis*-[VO(pic)$_2$(H$_2$O)] is correctly predicted by the "additivity rule" even though it has an axial carboxylate group bound to the $V^{IV}O$ ion: we believe that this apparent contradiction may be explained by considering the fact that the contribution to A_z of a carboxylate has been calculated for *cis*-[VO(oxalato)$_2$(H$_2$O)]$^{2-}$ (having an axial COO^-)[45] so that every possible reduction of A_z has probably been incorporated into this value.

Effect of an axial ligand on the structural and spectroscopic properties of a $V^{IV}O$ species: To obtain new insights into the effect of an axial ligand on the structural and spectroscopic properties of a $V^{IV}O$ species, several DFT simulations on the *trans*-[VO(6-mepic)$_2$(H_2O)] complex with the Gaussian 03 software were performed by varying the distance (R) between the vanadium atom and the water oxygen atom coordinated in the apical position in the range 2.1–3.8 Å, that is, from a value at which the interaction is very strong and comparable to that of the equatorial ligands to a value at which vanadium and water can be considered weakly interacting.

First, it would be interesting to evaluate how the energy of *trans*-[VO(6-mepic)$_2$(H_2O)] varies on increasing R from 2.1 to 3.8 Å. This is illustrated in Figure 6. As can be seen, the energy decreases from a maximum for $R=2.1$ Å to a minimum for $R=2.47$ Å, which indicates that the coordination of the axial water stabilises the structure, and then begins to increase again. A similar trend as a function of the distance V–N^{ax} has been found for the model of the non-haeme species $[Fe^{IV}O(NH_3)_5]^{2+}$.[46] However, as observed above, the energy varies little for distances between 2.3 and 2.6 Å, which are the distances observed experimentally for the V–L^{ax} interaction.

The variation of $|A_z|$, calculated with the Gaussian and ORCA software, as a function of R for *trans*-[VO(6-mepic)$_2$-(H_2O)] is presented in Figure 7. $|A_z|$ strongly suffers as a result of coordination of an axial ligand, changing from 146.2×10^{-4} cm^{-1} for $R=2.1$ Å to 159.0×10^{-4} cm^{-1} when $R=$ 3.8 Å through the value of 150.8×10^{-4} cm^{-1} at the equilibrium distance (see Tables S8 and S9 of the Supporting Information). The change in $|A_z|$ can be fitted by an exponential function described by $|A_z|^{calcd}=A[1-e^{-bR}]$, which approaches the value calculated for [VO(6-mepic)$_2$] when vanadium and the water molecule are at an infinite distance. Analogous results are obtained when the value of $|A_{iso}|^{calcd}$ is plotted as a function of R (Figure S14 of the Supporting Information). Note that, since other mathematical functions can reproduce the data, the exponential dependence must be considered a simple interpolation formula before its physical meaning is clarified.

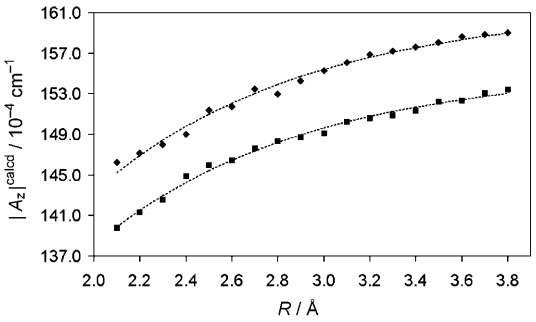

Figure 7. Variation of $|A_z|$ for the *trans*-[VO(6-mepic)$_2$(H_2O)] complex as a function of the distance V–OH_2 (R) calculated by Gaussian 03 (◆) and ORCA (■) software. The curves were fitted with the equations $|A_z|^{calcd}=161.48(1-e^{-1.09R})$ (dotted line) and $|A_z|^{calcd}=155.41(1-e^{-1.10R})$ (dotted line). R^2 values for the fitting are 0.987 and 0.993, respectively.

These interesting insights led us to examine the variation of other structural and spectroscopic properties, for example, the V=O, V–O and V–N distances, the O–V–O and N–V–N angles, the trigonality index τ, and the stretching frequency of V=O bond as a function of R. The results are represented in Figure 8 and in Table S10 and Figures S15–S21 of the Supporting Information. It appears that the variation of a certain property, ξ^{calcd}, follows the same trend as found for $|A_z|$ and $|A_{iso}|$ and can be interpolated by the function $\xi^{calcd}=A[1\pm e^{-bR}]$ in which the positive or negative sign depends on the increasing or decreasing character of the mathematical function. From these results it emerges that as the strength of the axial interaction in a $V^{IV}O$ species increases the bond distances V=O and V–L^{eq} should increase, both of the L^{eq}–V–L^{eq} angles should decrease and the distortion towards the trigonal bipyramid expressed by the trigonality index τ should increase. This is confirmed by comparison of the pentacoordinated structures of [VO(acetylacetonato)$_2$][28] and [VO{*N*,*N*′-ethylenebis(salicylideneaminato)}][47] with the corresponding octahedral species *trans*-[VO(acetylacetonato)$_2$(4-methylpyridine)][48] and *trans*-[VO{*N*,*N*′-bis(3-methoxysalicylidene)ethane-1,2-diaminato}(H_2O)][41] (see Table S11 of the Supporting Information).

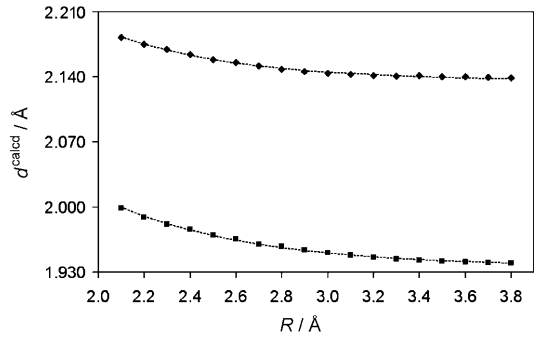

Figure 8. Variation of the V–N (◆) and V–O (■) bond lengths of the *trans*-[VO(6-mepic)$_2$(H_2O)] complex as a function of the distance V–OH_2 (R). The curves were fitted with the equations $d_{V-N}{}^{calcd}=2.135(1+e^{-1.814R})$ (dotted line) and $d_{V-O}{}^{calcd}=1.936(1+e^{-1.624R})$ (dotted line). R^2 values for the fitting are 0.995 and 0.998, respectively.

Another change that can be observed when the distance V–OH_2 is varied is the composition of the molecular orbital containing the single electron (SOMO). Although one could expect that in a $V^{IV}O$ complex the SOMO is principally a vanadium d_{xy}-based orbital, an analysis of its composition reveals that the presence of an axial ligand results in a mixture of vanadium d_{xy} and $d_{x^2-y^2}$ orbitals and that their mixing increases with decreasing R. The contributions to the SOMO of the sum of all the vanadium d orbitals and of the vanadium d_{xy} and $d_{x^2-y^2}$ orbitals are shown as a function of the distance V–OH_2 in Figure 9; it can be observed that, whereas the first contribution decreases slightly with R, the contributions of the vanadium d_{xy} and $d_{x^2-y^2}$ orbitals follow a

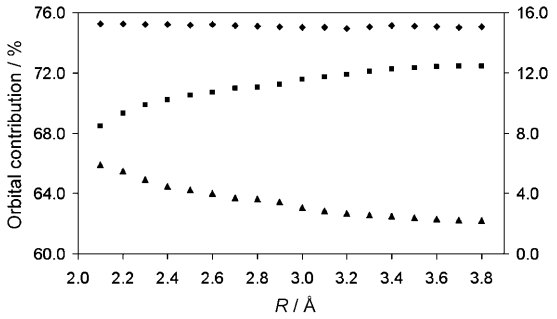

Figure 9. Calculated percent contributions to the SOMO of the sum of all the vanadium d orbitals (◆), the d_{xy} orbital (■) and the $d_{x^2-y^2}$ (▲) orbital for the *trans*-[VO(6-mepic)$_2$(H_2O)] complex as a function of the distance V–OH_2 (R). The left-hand axis refers to the vanadium d and d_{xy} orbital contributions, the right-hand axis to the vanadium $d_{x^2-y^2}$ orbital.

dependence similar to that found above for the other examined properties. This type of combination has also been observed for [VOCl(capca)] after coordination of the axial ligand.[26] The composition of the SOMO as a function of the distance V–OH_2 is shown in Table S12 of the Supporting Information.

Analysis of the electronic structure and molecular orbital composition: The electronic structure of the *trans* octahedral and square-pyramidal forms is strongly influenced by the change in the geometry after axial coordination of a water molecule. By going from the pentacoordinated structure of [VO(6-mepic)$_2$] to the hexacoordinated structure of *trans*-[VO(6-mepic)$_2$(H_2O)] the equatorial bond distances remain almost unchanged (differences below 1.8%), the pseudoaxial N–V–N bond angle changes from 156.8 to 164.9°, whereas the pseudoequatorial O–V–O angle undergoes the most important deformation from 126.5 to 144.9°; the value of parameter τ changes from 0.51 to 0.33 (Table 1). The increase in τ as a function of the distance V–OH_2 (R) is presented graphically in Figure S20 of the Supporting Information. Thus, the coordination of a water molecule *trans* to the V=O group results in the transformation of the structure distorted towards the trigonal bipyramid to a distorted octahedral with the arrangement of the oxo group and the four equatorial donors closer to the square pyramid.

The compositions of the most important occupied and virtual molecular orbitals (MO) of *trans*-[VO(6-mepic)$_2$(H_2O)] and [VO(6-mepic)$_2$] are given in Table 4 and the molecular orbitals of the octahedral species are shown in Figure 10. The electronic structures and molecular orbital compositions were analysed by choosing a coordinate system in which the V=O bond occupies the z axis with the pyridine nitrogen atoms roughly oriented along the x axis and the carboxylate oxygen atoms along the y axis. In both cases, of the vanadium d orbitals, d_{xy} is lower in energy than the other four and is the SOMO. The order of increasing energy of the five vanadium d-based MOs reflects that calculated by Ballhausen and Gray for a $V^{IV}O$ complex with C_{4v} symmetry:[49] $d_{xy} < d_{xz} \sim d_{yz} < d_{x^2-y^2} < d_{z^2}$. Differences in the covalency and donor strengths of the ligands as well as deviations from a perfect square-pyramidal geometry reduce the effective symmetry of the species from C_{4v}.

In the following discussion the electronic structure of the [VO(6-mepic)$_2$] fragment and the changes that arise when the water molecule interacts with it axially, occupying the sixth coordination position, are described. A favourable π interaction between the vanadium d_{xy} and oxygen p_x orbitals of the two bound carboxylate oxygen atoms lowers the vanadium character of the SOMO to around 76% in both the penta- and hexacoordinated species. The vanadium d_{xz}- and d_{yz}-based MOs are engaged in a strong π bond with the O_{oxo} p_x and p_y orbitals (this can be observed in Figure 10 for *trans*-[VO(6-mepic)$_2$(H_2O)]) with the consequence that their

Table 4. Percent composition of the highest occupied and lowest unoccupied molecular orbitals of *trans*-[VO(6-mepic)$_2$(H_2O)] and [VO(6-mepic)$_2$].

	trans-[VO(6-mepic)$_2$(H_2O)]								[VO(6-mepic)$_2$]						
Orbital	E [eV]	V (tot)	V (d)	O_{oxo}	COO^-	Pyr	H_2O	Main character	E [eV]	V (tot)	V (d)	O_{oxo}	COO^-	Pyr	Main Character
LUMO+8	0.59	42.9	33.1	16.7	6.4	23.5	5.7	$3d_{z^2}$	0.69	46.7	0.8	0.4	1.0	45.7	4*s*
LUMO+7	0.16	25.6	10.8	4.0	1.1	3.6	65.3	$\sigma^*_{H_2O}$	−0.05	56.5	53.2	19.5	3.4	18.7	$3d_{z^2}$
LUMO+6	−0.13	77.3	75.5	0.3	8.2	13.1	0.5	$3d_{x^2-y^2}$	−0.53	71.7	71.1	4.6	12.3	10.9	$3d_{x^2-y^2}$
LUMO+5	−0.78	66.6	66.6	18.5	6.9	7.2	0.1	$3d_{yz}$	−0.63	68.9	68.8	17.4	9.8	3.3	$3d_{yz}$
LUMO+4	−1.02	39.2	39.1	10.2	0.5	46.5	0.0	$3d_{xz}$	−1.19	43.1	43.0	11.4	0.5	41.7	$3d_{xz}$
LUMO+3	−1.29	0.2	0.1	0.0	6.6	89.5	0.1	π^*_{pyr}	−1.49	0.4	0.4	0.1	6.7	89.1	π^*_{pyr}
LUMO+2	−1.43	26.2	26.1	9.3	10.8	52.4	0.3	π^*_{pyr}	−1.62	21.2	21.1	7.5	11.0	59.0	π^*_{pyr}
LUMO+1	−2.05	1.4	1.3	0.8	14.2	82.1	0.4	π^*_{pyr}	−2.27	7.7	7.6	5.1	10.0	76.2	π^*_{pyr}
LUMO	−2.06	9.0	8.9	6.2	9.9	74.0	0.0	π^*_{pyr}	−2.33	3.3	3.0	2.1	15.7	77.9	π^*_{pyr}
HOMO	−6.22	76.2	75.2	0.6	16.7	5.8	0.0	$3d_{xy}$	−6.43	76.0	75.3	0.4	16.8	6.0	$3d_{xy}$
HOMO-1	−7.10	0.5	0.4	0.1	86.7	12.4	0.0	$O^{lp}_{COO^-}$	−7.37	0.4	0.3	0.9	86.6	11.7	$O^{lp}_{COO^-}$
HOMO-2	−7.22	7.9	7.9	0.2	81.1	10.3	0.1	$O^{lp}_{COO^-}$	−7.47	8.3	8.2	0.0	81.2	10.1	$O^{lp}_{COO^-}$
HOMO-3	−7.53	0.4	0.3	0.3	37.9	55.9	0.5	π_{pyr}	−7.77	0.2	0.2	0.9	24.1	68.7	π_{pyr}
HOMO-4	−7.53	0.3	0.2	5.1	50.7	40.5	0.5	$\pi_{COO^-}+\pi_{pyr}$	−7.79	0.0	0.0	0.0	16.8	76.9	π_{pyr}
HOMO-5	−7.68	0.6	0.4	14.7	38.1	41.7	0.3	$\pi_{pyr}+O^{lp}_{COO^-}$	−7.99	0.6	0.3	18.0	73.4	6.6	π_{COO^-}
HOMO-6	−7.89	0.4	0.3	0.8	61.9	33.1	1.6	$O^{lp}_{COO^-}$	−8.23	0.9	0.5	7.5	66.3	24.0	π_{COO^-}
HOMO-7	−8.04	1.3	0.5	5.9	71.8	18.8	0.5	$O^{lp}_{COO^-}$	−8.33	1.3	0.4	12.3	69.5	16.1	$O^{lp}_{COO^-}$
HOMO-8	−8.42	8.3	8.0	23.3	7.8	59.8	0.0	π_{pyr}	−8.73	5.8	5.5	20.8	4.7	68.0	π_{pyr}

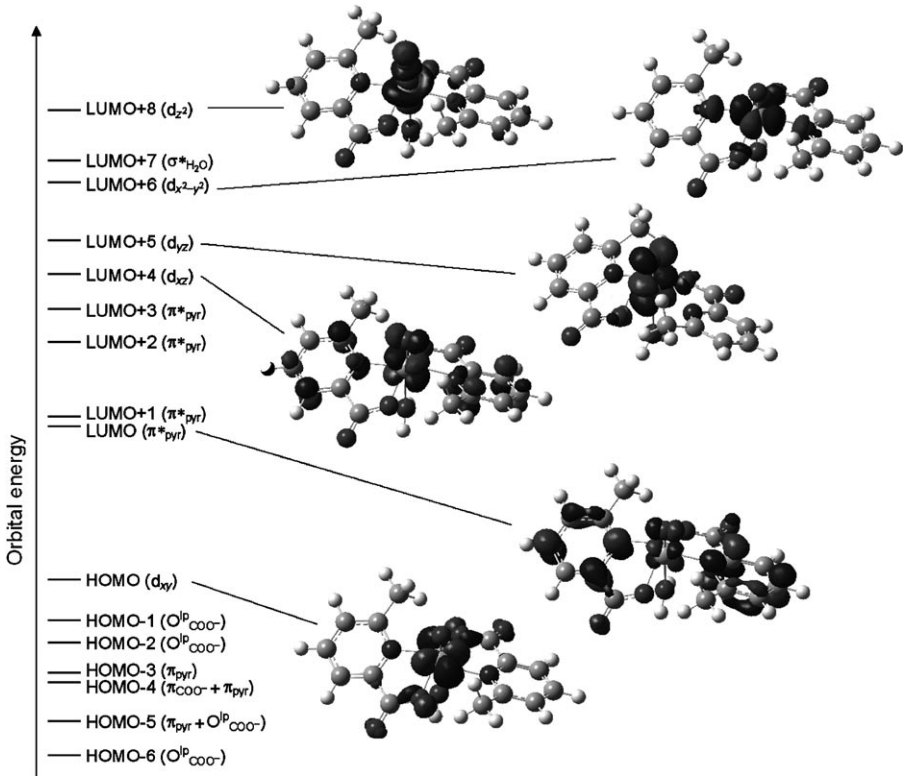

Figure 10. Molecular orbital diagram for *trans*-[VO(6-mepic)$_2$(H$_2$O)]. Note that the energy levels are not drawn to scale.

energy is higher than the vanadium d_{xy} orbital by approximately 5.2 and 5.6 eV (5.2 and 5.4 eV for *trans*-[VO(6-mepic)$_2$(H$_2$O)]). Such a π interaction shows a significant degree of covalency, as evidenced by the low contribution of vanadium d orbitals to the MOs (Table 4). The two higher-energy vanadium $d_{x^2-y^2}$ and d_{z^2} orbitals are antibonding between the vanadium and the equatorial donors on the one hand, and the vanadium and oxo group and pyridine ring on the other (see Figure 10 for *trans*-[VO(6-mepic)$_2$(H$_2$O)]).

The axial bonding of the water molecule with [VO(6-mepic)$_2$] provides interesting insights into the change in the energy levels as a consequence of the transformation from the square-pyramidal to the octahedral complex; this is illustrated in Figure 11. The two lone pairs of the H$_2$O ligand

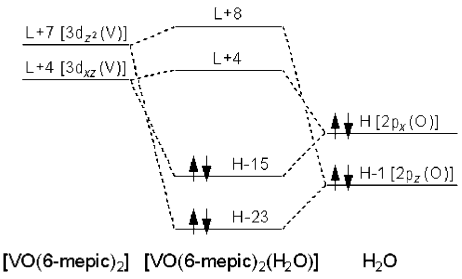

Figure 11. Interactions between molecular orbitals with the same symmetry belonging to [VO(6-mepic)$_2$] and H$_2$O fragments.

are situated in the O_{water} p_z- and p_x-based MOs, which have σ and π symmetry. Therefore the O_{water} p_z orbital can interact with the vanadium d_{z^2} orbital, whereas the O_{water} p_x orbital overlaps with the vanadium d_{xz} orbital: this results in a smaller energy difference between the vanadium d_{xz} and d_{yz} orbitals from [VO(6-mepic)$_2$] (0.56 eV) to *trans*-[VO(6-mepic)$_2$(H$_2$O)] (0.24 eV). It is also possible that the concomitant decrease in τ, which should be accompanied by an approaching of the vanadium d_{xz} and d_{yz} levels,[50] may amplify this effect. The axial interaction with the O_{water} p_z orbital of the water molecule pushes up the energy of the vanadium d_{z^2} orbital by 0.64 eV.

Conclusion

The previously unreported equilibrium between the penta-coordinated square-pyramidal and the hexacoordinated *trans* octahedral forms of $V^{IV}O$ complexes formed by bidentate ligands with (N,O) or (O,O) donor sets has been described. The octahedral species are countersigned by experimental absolute values of the ^{51}V hyperfine coupling constants along the z axis ($|A_z|^{exptl}$) that are significantly lower than those predicted on the basis of the "additivity rule",[16,17] which can be attributed to the presence of a donor axially bound to the $V^{IV}O$ ion. DFT calculations allow the structures and A_z values to be predicted with a good degree of accuracy and therefore to distinguish a penta- from a hexacoordinated complex with a water or solvent molecule *trans* to the V=O group. The best agreement between the calculated (A_z^{calcd}) and experimental (A_z^{exptl}) values can be obtained by using a half-and-half hybrid functional, for example, BHandHLYP, with the 6-311g(d,p) basis set, or with the PBE0 functional and the VTZ set considering the second-order spin–orbit contribution to the ***A*** tensor. These two options can be accomplished by using the Gaussian 03 and ORCA software, respectively.[38,40]

From the results of this work it emerges that such an equilibrium could be more frequent than had been believed, as demonstrated by analysis of the systems containing dipyridin-2-ylmethanol and 1,2-dimethyl-3-hydroxy-4(1*H*)-pyridinone. It should not be surprising if such an equilibrium was also observed with other metal ions similar to $V^{IV}O^{2+}$, for example, $Cr^{V}O^{3+}$ and $Mo^{V}O^{3+}$.

Of course most of the $V^{IV}O$ species are square-pyramidal: a search in the Cambridge Structural Database[34] for bidentate (N,O) and (O,O) ligands gives 35 and 30 hits, respectively, and of these, only two and five structures are characterised by a *trans* octahedral arrangement. Interestingly, for the (N,O) ligands, the two octahedral structures are formed by two picolinic derivatives, 6-ethylpicolinic and quinaldic acid.[23,29] The "additivity rule" can be successfully applied to all the pentacoordinated complexes. However, the presence of an axial ligand (charged or not) can change the A_z value, which suggests that the statement that axial ligands do not contribute to the A_z value must be revised. In such situations DFT methods can help to predict A_z values and demonstrate the presence of a ligand *trans* to the V=O group.

The decrease in $|A_z|$ after the axial binding to $V^{IV}O$ ion of a sixth donor is mainly due to the reduction in $|A_{iso}|$. Tolis et al. proposed for the [VOCl(capca)] and [VO(NCS)(capca)] complexes that the negative axial charge induces a radial expansion of the vanadium d_{xy} orbital, which results in reduced electron density on the metal and in a lowering of $|A_z|^{exptl}$.[19] As is known from EPR theory, the isotropic hyperfine coupling constant A_{iso} is directly proportional to the spin density at the point of the corresponding nucleus ($\rho_N^{\alpha-\beta}$). In the traditional interpretations, $\rho_N^{\alpha-\beta}$ is frequently approximated by the density of the singly occupied molecular orbital. However, this simple approach is not sufficient to explain the high value of $|A_{iso}|$ for transition-metal complexes in which the unpaired electron occupies metal d orbitals that have a node at the nucleus. This apparent contradiction can be understood if the interaction of the unpaired electron with the other electrons of the system is taken into account; such an interaction spin-polarises the electron distribution in both the core and valence shells.[51,52] Some year ago, Kaupp and co-workers showed that the spin polarisation enhances the exchange interaction of the 2s and 2p shells with the singly occupied orbital contributing with a negative sign to A_{iso}.[53] It is plausible that a mechanism of this type is also operative for the $V^{IV}O$ complexes discussed in this report. This possibility is confirmed by the good agreement between the $|A_{iso}|^{calcd}$ and $|A_{iso}|^{exptl}$ values if the half-and-half hybrid functionals, which reproduce well the core–shell spin polarisation, are used. To prove this assumption, an analysis of the spin distribution and of the various contributions to $\rho_N^{\alpha-\beta}$ for the $V^{IV}O$ complexes is in progress.

The variation of the structural (V=O, V−O and V−N distances, O−V−O and N−V−N angles, and the trigonality index τ) and spectroscopic ($|A_z|$, $|A_{iso}|$ and ν(V=O)) properties of *trans*-[VO(6-mepic)$_2$(H_2O)] as a function of the distance V−OH_2 (R) follows a similar functional dependence, which approaches the value measured for pentacoordinated square-pyramidal species when the distance is infinite. We believe that these results could be of general validity and our intention is to confirm this hypothesis with other transition-metal complexes.

The results discussed in this work may be helpful for interpreting EPR spectra and identifying the coordination sphere of $V^{IV}O$ complexes present in biological systems when the possibility of an apical ligand binding to vanadium must be taken into account. For example, the presence of a lysine and an imidazole nitrogen atom in the axial position has been suggested for the vanadyl-substituted chloroplast F_1-ATPase (CF_1) and in the reduced inactive form of vanadium bromoperoxidase (VBrPO), respectively.[18a,54]

Experimental and Computational Details

Chemicals: 6-Methylpicolinic and 6-methyl-2,3-pyridinedicarboxylic acids and 1,2-dimethyl-3-hydroxy-4(1*H*)-pyridinone were Aldrich products of puriss. quality. Dipyridin-2-ylmethanol was obtained by reduction of dipyridin-2-yl ketone according to the established methods.[55] $V^{IV}O$ solutions were prepared with $VOSO_4{\cdot}3H_2O$ by following the procedure described in the literature.[56] All operations were performed under a purified argon atmosphere to avoid oxidation of the $V^{IV}O$ ion.

Preparation of the [VO(6-mepic)$_2$] complex: [VO(6-mepic)$_2$] was prepared by dissolving stoichiometric amounts of $VOSO_4{\cdot}3H_2O$ and 6-methylpicolinic acid in water, adjusting the pH value to 5 with a diluted solution of NaOH and heating at reflux for about 1 h. The solid formed was filtered when the solution was still warm and dried in vacuo over P_2O_5. Elemental analysis calcd (%) for $C_{14}H_{12}N_2O_5V$ (339.20): C 49.57, H 3.57, N 8.26, H_2O 0.0, V_2O_5 26.8; found: C 49.45, H 3.35, N 8.34, H_2O 0.0, V_2O_5 26.0.

Spectroscopic and analytical measurements: The EPR spectra were recorded with an X-band (9.15 GHz) Varian E-9 spectrometer at 120 K (anisotropic spectra) or at room temperature (isotropic spectra). The experimental A values were determined by simulations using the computer suite program Bruker WinEPR/SimFonia.[57] Elemental analyses (C, H, N) were performed with a Perkin–Elmer 240 B analyser. The thermogravimetric studies, to determine the V_2O_5 and H_2O content, were carried out with a Perkin–Elmer TGS-2 instrument under a nitrogen atmosphere.

The intensities of the EPR signals used to determine K_c values for the equilibria between the square-pyramidal and octahedral forms of the bischelated species formed by 6-methyl-2,3-dicarboxylic acid and dipyridin-2-ylmethanol were measured in the $M_I=-7/2$ parallel transition by double integration of the first derivative spectra. The uncertainty of each point was calculated to be approximately 10% of the value of K_c. The resonances at high-field ($M_I=7/2$) were not suitable for the evaluation of the values of K_c because of broadening of the linewidth with increasing magnetic field, which makes it difficult to quantify the amount of the *trans* octahedral species at high ionic strength.

DFT calculations: All the calculations presented in this paper were performed by DFT methods[58] using the Gaussian 03 (revision C.02)[38] or ORCA (version 2.6.35) programs.[40] The hybrid exchange-correlation B3LYP,[59,60] the half-and-half BHandHLYP functional, as incorporated in the Gaussian 03, and the hybrid PBE0 functional[61] were used. The BHandHLYP functional includes a mixture of exact Hartree–Fock and DFT methods to calculate the exchange-correlation energy by using the expression $E_{XC}=0.5E_X^{HF}+0.5E_X^{LSDA}+0.5E_X^{B}+E_C^{LYP}$ in which E_X^{HF}, E_X^{LSDA}, E_X^{B} and E_C^{LYP} are the energies due to the Hartree–Fock exchange, the local spin density approximation (LSDA) exchange functional, the gradient-corrected Becke 88 (B) exchange functional, and the gradient-corrected Lee–Yang–Parr (LYP) correlation functional, respectively. Previous attempts to change the percentage of the several components in the BHandHLYP functional did not significantly improve the prediction of A_z. The HF method may be regarded as a special case of DFT in which the exchange is treated exactly and the correlation is completely neglected.[58] It has been shown that the Hartree–Fock method is significantly inferior to DFT approaches for predicting all EPR parameters, mainly because it overestimates the bond ionicity in polar bonds, which results in an incorrect description of the spin polarisation by which spin density could be transferred to orbitals with s character.[36a]

All the geometries of the $V^{IV}O$ complexes investigated were first preoptimised at the B3LYP/sto-3g level of theory and further optimised at the B3LYP/6-311g(d) level of theory in the gas phase using Gaussian 03 software. For all the structures, minima were verified by frequency calculations. Because it has been widely demonstrated in the literature that the optimisation of a transition-metal complex in the gas phase is enough to obtain a good agreement between experimental and simulated EPR parameters[26,36a,37,39] and our goal is to demonstrate only in a qualitatively way that the axial coordination of a solvent molecule can reduce the value of $|A_z|$, no calculations in solution were performed. This limitation, however, must be kept in mind.

The optimised structures were used to calculate the ^{51}V hyperfine coupling constants (A_{iso}, A_x, A_y and A_z) at the BHandHLYP/6-311g(d,p) level of theory using Gaussian 03 and at the PBE0/VTZ level of theory using ORCA. A_{iso} and A_z values (as are A_x and A_y) are negative, but their absolute values are usually reported in the literature. This must kept in mind when positive values are discussed. The percent deviation from the absolute experimental value $|A_z|^{exptl}$ was calculated from $100[(|A_z|^{calcd}-|A_z|^{exptl})/|A_z|^{exptl}]$ (see Tables 2 and 3).

The stretching frequency of V=O (ν(V=O)) bond was simulated at the B3LYP/6-311g(d) level of theory.

The molecular orbital (MO) composition was analysed in terms of the atomic orbitals or groups of atoms by using the AOMix program (revision 6.46).[62]

Theoretical background: The "additivity rule" affirms that for a $V^{IV}O$ complex the ^{51}V isotropic hyperfine coupling constants measured in solution at room temperature (A_{iso}) and ^{51}V anisotropic hyperfine coupling constants along the z axis measured on a polycrystalline powder or on a frozen sample (A_z) can be calculated from the sum of the contributions of each equatorial donor[16,17] [Eqs. (3) and (4)].

$$A_{iso}=\sum_{i=1}^{4}A_{iso}(\text{donor}i)=A_{iso}(\text{donor1})+A_{iso}(\text{donor2})+A_{iso}(\text{donor3})+A_{iso}(\text{donor4}) \quad (3)$$

$$A_z=\sum_{i=1}^{4}A_z(\text{donor}i)=A_z(\text{donor1})+A_z(\text{donor2})+A_z(\text{donor3})+A_z(\text{donor4}) \quad (4)$$

Such an empirical rule allows a correlation of A_{iso} or A_z with the number and types of ligands in the equatorial plane of the $V^{IV}O$ ion and has been proved and accepted in a large number of works. The contribution to A_{iso} or A_z has an approximately inverse relationship with the electron-donating capacity of the ligand, with the most donating ligands contributing the least to the coupling constant. Experimental $|A_z|$ or $|A_{iso}|$ values fall in the range of $\sim 3\times10^{-4}$ cm^{-1} with respect to the value calculated with Equations (3) and (4).[16,17] In fact, the analysis of the anisotropic EPR spectra is preferred to that of the isotropic spectra because they allow more detailed information to be obtained on 1) the symmetry and coordination geometry of the $V^{IV}O$ species, 2) the identity of the equatorial ligands because the A_z value is more sensitive to equatorial donors than A_{iso} and 3) the presence of minor species in solution, which cannot be detected from examination of the isotropic spectra.

The $V^{IV}O$ ion has a d^1 electronic configuration with one unpaired electron. The hyperfine coupling constants in the EPR spectra arise from the interaction between the spin-angular momentum of the electron ($S=^1/_2$) with the spin-angular momentum of the ^{51}V nucleus ($I=^7/_2$, 99.8% natural abundance). The ^{51}V hyperfine coupling tensor $\boldsymbol{A}$ has three contributions: the isotropic Fermi contact (A^{FC}), the anisotropic or dipolar hyperfine interaction ($\boldsymbol{A}^{D}$) and the second-order effect that arises from spin–orbit coupling ($\boldsymbol{A}^{SO}$)[40] [Eq. (5), in which $\mathbf{1}$ is the unit tensor]. Here $\mathbf{1}$ is the unit tensor. A^{FC} and the components $A^{D}_{\mu\nu}$ and $A^{SO}_{\mu\nu}$ of the tensors $\boldsymbol{A}^{D}$ and $\boldsymbol{A}^{SO}$ are given by Equations (6)–(8). g_e and g_N are the g factors of the free electron and the nucleus, β_e and β_N the electron and nuclear magnetons, $\langle S_z\rangle$ the expectation value of the electronic spin on the z axis, $\rho_N^{\alpha-\beta}$ the spin density at the nucleus, $P_{k,l}^{\alpha-\beta}$ the spin density matrix, $\boldsymbol{r}$ the distance between the unpaired electron and the nucleus and h_v^{SOC} the spatial part of an effective one-electron spin–orbit operator.

$$\boldsymbol{A}=A^{FC}\mathbf{1}+\boldsymbol{A}^{D}+\boldsymbol{A}^{SO} \quad (5)$$

$$A^{FC}=\frac{4\pi}{3}g_e g_N\beta_e\beta_N\langle S_z\rangle^{-1}\rho_N^{\alpha-\beta} \quad (6)$$

$$A^{D}_{\mu\nu}=\frac{1}{2}g_e g_N\beta_e\beta_N\sum_{k,l}P_{k,l}^{\alpha-\beta}\left\langle\Phi_k\left|\frac{\boldsymbol{r}^2\delta_{\mu\nu}-3\boldsymbol{r}_\mu\boldsymbol{r}_\nu}{\boldsymbol{r}^5}\right|\Phi_l\right\rangle \quad (7)$$

$$A^{SO}_{\mu\nu}=\frac{1}{2S}g_e g_N\beta_e\beta_N\sum_{k,l}\frac{\partial P_{k,l}^{\alpha-\beta}}{\partial I_\mu}\langle\Phi_k|h_v^{SOC}|\Phi_l\rangle \quad (8)$$

The tensor $\boldsymbol{A}^{D}$ is always traceless: A_x^{D}, A_y^{D} and A_z^{D} are the elements of the diagonalised tensor, their sum being zero [Eq. (9)].

$$A_x^{D}+A_y^{D}+A_z^{D}=0 \quad (9)$$

The values of the ^{51}V anisotropic hyperfine coupling constants along the x, y and z axes are determined from Equations (10)–(12).

$$A_x=A^{FC}+A_x^{D}+A_x^{SO} \quad (10)$$

$$A_y=A^{FC}+A_y^{D}+A_y^{SO} \quad (11)$$

$$A_z=A^{FC}+A_z^{D}+A_z^{SO} \quad (12)$$

The value of A_z calculated with Equation (12) (A_z^{calcd}) can be compared with that expected on the basis of the "additivity rule" (A_z^{expct}) and with the experimental value (A_z^{exptl}); see Tables 2 and 3.

The value of A_{iso} can be calculated from Equation (13).

$$A_{iso}=\frac{1}{3}(A_x+A_y+A_z)=A^{FC}+\frac{1}{3}(A_x^{SO}+A_y^{SO}+A_z^{SO}) \quad (13)$$

By using Gaussian 03, which neglects the terms $A^{SO}_{\mu\nu}$, A_{iso} coincides with A^{FC} [Eq. (14)].

$$A_{iso}=\frac{1}{3}(A_x+A_y+A_z)=A^{FC} \quad (14)$$

[1] a) D. C. Crans, J. J. Smee, E. Gaidamauskas, L. Yang, *Chem. Rev.* **2004**, *104*, 849–902; b) D. Rehder, *Bioinorganic Vanadium Chemistry*, Wiley, New York, **2008**.

[2] a) H. Vilter in *Metal Ions in Biological Systems, Vol. 31* (Eds.: A. Sigel, H. Sigel), Marcel Dekker, New York, **1995**, pp. 325–362; b) V. L. Pecoraro, C. A. Slebodnick, B. J. Hamstra in *Vanadium Compounds: Chemistry, Biochemistry and Therapeutic Applications* (Eds.: A. S. Tracey, D. C. Crans), ACS, Washington, **1998**, pp. 157–167.

[3] a) R. L. Robson, R. R. Eady, T. J. Richardson, R. W. Miller, M. Hawkins, J. R. Postgate, *Nature* **1986**, *322*, 388–390; b) R. R. Eady in *Vanadium Compounds: Chemistry, Biochemistry and Therapeutic Applications* (Eds.: A. S. Tracey, D. C. Crans), ACS, Washington, **1998**, pp. 363–405; c) R. R. Eady, *Coord. Chem. Rev.* **2003**, *237*, 23–30.

[4] a) L. Josephson, L. C. Cantley, Jr., *Biochemistry* **1977**, *16*, 4572–4578; b) L. C. Cantley, Jr., L. Josephson, R. Warner, M. Yanagisawa, C. Lechene, G. Guidotti, *J. Biol. Chem.* **1977**, *252*, 7421–7423; c) M. J. Gresser, A. S. Tracey in *Vanadium in Biological Systems* (Ed.: N. D. Chasteen), Kluwer Academic, Dordrecht, **1990**, pp. 63–79; d) P. J. Stankiewicz, A. S. Tracey, D. C. Crans in *Metal Ions in Biological Systems, Vol. 31* (Eds.: A. Sigel, H. Sigel), Marcel Dekker, New York, **1995**, pp. 287–324, and references therein.

[5] a) E. L. Tolman, E. Barris, M. Burns, A. Pansini, R. Partridge, *Life Sci.* **1979**, *25*, 1159–1164; b) Y. Shechter, S. J. D. Karlish, *Nature* **1980**, *284*, 556–558; c) K. H. Thompson, J. H. McNeill, C. Orvig,

Chem. Rev. **1999**, *99*, 2561–2571, and references therein; d) K. H. Thompson, C. Orvig, *Coord. Chem. Rev.* **2001**, *219–221*, 1033–1053, and references therein; e) Y. Shechter, I. Goldwaser, M. Mironchik, M. Fridkin, D. Gefel, *Coord. Chem. Rev.* **2003**, *237*, 3–11; f) K. Kawabe, Y. Yoshikawa, Y. Adachi, H. Sakurai, *Life Sci.* **2006**, *78*, 2860–2866.

[6] a) F. H. Nielsen in *Metal Ions in Biological Systems, Vol. 31* (Eds.: A. Sigel, H. Sigel), Marcel Dekker, New York, **1995**, pp. 543–573; b) F. H. Nielsen in *Vanadium Compounds: Chemistry, Biochemistry and Therapeutic Applications* (Eds.: A. S. Tracey, D. C. Crans), ACS, Washington, **1998**, pp. 297–315.

[7] K. Kustin, W. E. Robinson in *Metal Ions in Biological Systems, Vol. 31* (Eds.: A. Sigel, H. Sigel), Marcel Dekker, New York, **1995**, pp. 511–542.

[8] T. Kiss, T. Jakusch, D. Hollender, A. Dörnyei, E. A. Enyedy, J. Costa Pessoa, H. Sakurai, A. Sanz-Medel, *Coord. Chem. Rev.* **2008**, *252*, 1153–1162, and references therein.

[9] P. Caravan, L. Gelmini, N. Glover, F. G. Herring, H. Li, J. H. McNeill, S. J. Rettig, I. A. Setyawati, E. Shuter, Y. Sun, A. S. Tracey, V. G. Yuen, C. Orvig, *J. Am. Chem. Soc.* **1995**, *117*, 12759–12770.

[10] a) G. R. Hanson, Y. Sun, C. Orvig, *Inorg. Chem.* **1996**, *35*, 6507–6512; b) P. Buglyó, E. Kiss, I. Fábián, T. Kiss, K. Petrohán, D. Sanna, E. Garribba, G. Micera, *Inorg. Chim. Acta* **2000**, *306*, 174–183.

[11] B. D. Liboiron, K. H. Thompson, G. R. Hanson, E. Lam, N. Aebischer, C. Orvig, *J. Am. Chem. Soc.* **2005**, *127*, 5104–5115.

[12] M. Rangel, A. Tamura, C. Fukushima, H. Sakurai, *J. Biol. Inorg. Chem.* **2001**, *6*, 128–132.

[13] D. Sanna, G. Micera, E. Garribba, *Inorg. Chem.* **2010**, *49*, 174–187.

[14] a) C. D. Garner, D. Collison, F. E. Mabbs in *Metal Ions in Biological Systems, Vol. 31* (Eds.: A. Sigel, H. Sigel), Marcel Dekker, New York, **1995**, pp. 617–670; b) G. Micera, D. Sanna in *Vanadium in the Environment Part 1: Chemistry and Biochemistry* (Ed.: J. O. Nriagu), Wiley, New York, **1998**, pp. 131–166.

[15] K. Wüthrich, *Helv. Chim. Acta* **1965**, *48*, 1012–1017.

[16] N. D. Chasteen in *Biological Magnetic Resonance, Vol. 3* (Eds.: L. J. Berliner, J. Reuben), Plenum Press, New York, **1981**, pp. 53–119.

[17] T. S. Smith II, R. LoBrutto V. L. Pecoraro, *Coord. Chem. Rev.* **2002**, *228*, 1–18.

[18] a) B. J. Hamstra, A. P. L. Houseman, G. J. Colpas, J. W. Kampf, R. LoBrutto, W. D. Frasch, V. L. Pecoraro, *Inorg. Chem.* **1997**, *36*, 4866–4874; b) T. Jakusch, P. Buglyó, A. I. Tomaz, J. Costa Pessoa, T. Kiss, *Inorg. Chim. Acta* **2002**, *339*, 119–128; c) E. Garribba, E. Lodyga-Chruscinska, G. Micera, A. Panzanelli, D. Sanna, *Eur. J. Inorg. Chem.* **2005**, 1369–1382, and references therein.

[19] a) E. J. Tolis, K. D. Soulti, C. P. Raptopoulou, A. Terzis, Y. Deligiannakis, T. A. Kabanos, *J. Chem. Soc. Chem. Commun.* **2000**, 601–602; b) E. J. Tolis, V. I. Teberekidis, C. P. Raptopoulou, A. Terzis, M. Sigalas, Y. Deligiannakis, T. A. Kabanos, *Chem. Eur. J.* **2001**, *7*, 2698–2710.

[20] M. T. Cocco, V. Onnis, G. Ponticelli, B. Meier, D. Rehder, E. Garribba, G. Micera, *J. Inorg. Biochem.* **2007**, *101*, 19–29.

[21] a) H. Sakurai, K. Fujii, S. Fujimoto, Y. Fujisawa, K. Takechi, H. Yasui in *Vanadium Compounds: Chemistry, Biochemistry and Therapeutic Applications* (Eds.: A. S. Tracey, D. C. Crans), ACS, Washington, **1998**, pp. 344–352; b) H. Sakurai in *Vanadium: the Versatile Metal* (Eds.: K. Kustin, J. Costa Pessoa, D. C. Crans), ACS, Washington, **2007**, pp. 110–120.

[22] E. Kiss, E. Garribba, G. Micera, T. Kiss, H. Sakurai, *J. Inorg. Biochem.* **2000**, *78*, 97–108.

[23] T. Sasagawa, Y. Yoshikawa, K. Kawabe, H. Sakurai, Y. Kojima, *J. Inorg. Biochem.* **2002**, *88*, 108–112.

[24] E. Kiss, D. Petrohán, D. Sanna, E. Garribba, G. Micera, T. Kiss, *Polyhedron* **2000**, *19*, 55–61.

[25] a) J. Gätjens, B. Maier, T. Kiss, E. M. Nagy, P. Buglyó, H. Sakurai, K. Kawabe, D. Rehder, *Chem. Eur. J.* **2003**, *9*, 4924–4935; b) J. Gätjens, B. Meier, Y. Adachi, H. Sakurai, D. Rehder, *Eur. J. Inorg. Chem.* **2006**, 3575–3585.

[26] C. P. Aznar, Y. Deligiannakis, E. J. Tolis, T. A. Kabanos, M. Brynda, R. D. Britt, *J. Phys. Chem. A* **2004**, *108*, 4310–4321.

[27] a) R. G. Wilkins, R. Yelin, D. W. Margerum, D. C. Weatherbum, *J. Am. Chem. Soc.* **1969**, *91*, 4326–4326; b) R. Barbucci, L. Fabbrizzi, P. Paoletti, A. Vacca, *J. Chem. Soc. Dalton Trans.* **1973**, 1763–1767; c) P. Paoletti, L. Fabbrizzi, R. Barbucci, *Inorg. Chim. Acta Rev.* **1973**, *7*, 43–68; d) F. P. Hinz, D. W. Margerum, *Inorg. Chem.* **1974**, *13*, 2941–2949; e) A. Anichini, L. Fabbrizzi, P. Paletti, R. M. Clay, *Inorg. Chim. Acta* **1977**, *24*, L21–L23 and references therein; f) E. Iwamoto, T. Kamamaru, Y. Sumitomo, Y. Suzuki, J. Nishimoto, *J. Chem. Soc. Faraday Trans.* **1995**, *91*, 627–630.

[28] E. Shuter, S. J. Rettig, C. Orvig, *Acta Crystallogr. Sect. C* **1995**, *51*, 12–14, and references therein.

[29] N Okabe, Y. Muranishi, *Acta Crystallogr. Sect. E* **2002**, *58*, m287–m289.

[30] E. Lodyga-Chruscinska, G. Micera, E. Garribba, unpublished results.

[31] a) S. Fujimoto, K. Fujii, H. Yasui, R. Matsushita, J. Takada, H. Sakurai, *J. Clin. Biochem. Nutr.* **1997**, *23*, 113–129; b) H. Sakurai, Y. Fujisawa, S. Fujimoto, H. Yasui, T. J. Takino, *J. Trace Elem. Exp. Med.* **1999**, *12*, 393–401.

[32] L. Pisano, D. Kiss, K. Várnagy, D. Sanna, G. Micera, E. Garribba, *Eur. J. Inorg. Chem.* **2009**, 2362–2374.

[33] a) P. Buglyó, T. Kiss, D. Sanna, E. Garribba, G. Micera, *J. Chem. Soc. Dalton Trans.* **2002**, 2275–2282; b) M. Rangel, A. Leite, M. J. Amorim, E. Garribba, G. Micera, E. Lodyga-Chruscinska, *Inorg. Chem.* **2006**, *45*, 8086–8097.

[34] F. H. Allen, O. Kennard, *Chem. Des. Autom. News* **1993**, *8*, 31–37.

[35] E. Lodyga-Chruscinska, D. Sanna, E. Garribba, G. Micera, *Dalton Trans.* **2008**, 4903–4916.

[36] a) *Calculation of NMR and EPR Parameters. Theory and Applications* (Eds.: M. Kaupp, M. Bühl, V. G. Malkin), Wiley-VCH, Weinheim, **2004**; b) C. Remenyi, R. Reviakine, A. V. Arbuznikov, J. Vaara, M. Kaupp, *J. Phys. Chem. A* **2004**, *108*, 5026–5033, and references therein; c) F. Neese, *Coord. Chem. Rev.* **2009**, *253*, 526–573.

[37] a) M. L. Munzarová, M. Kaupp, *J. Phys. Chem. B* **2001**, *105*, 12644–12652, and references therein; b) A. C. Saladino, S. C. Larsen, *J. Phys. Chem. A* **2003**, *107*, 1872–1878; c) F. Neese, *J. Chem. Phys.* **2003**, *118*, 3939–3948; d) A. C. Saladino, S. C. Larsen, *Catal. Today* **2005**, *105*, 122–133, and references therein.

[38] Gaussian 03, Revision C.02, M. J. Frisch, G. W. Trucks, H. B. Schlegel, G. E. Scuseria, M. A. Robb, J. R. Cheeseman, J. A. Montgomery, Jr., T. Vreven, K. N. Kudin, J. C. Burant, J. M. Millam, S. S. Iyengar, J. Tomasi, V. Barone, B. Mennucci, M. Cossi, G. Scalmani, N. Rega, G. A. Petersson, H. Nakatsuji, M. Hada, M. Ehara, K. Toyota, R. Fukuda, J. Hasegawa, M. Ishida, T. Nakajima, Y. Honda, O. Kitao, H. Nakai, M. Klene, X. Li, J. E. Knox, H. P. Hratchian, J. B. Cross, C. Adamo, J. Jaramillo, R. Gomperts, R. E. Stratmann, O. Yazyev, A. J. Austin, R. Cammi, C. Pomelli, J. W. Ochterski, P. Y. Ayala, K. Morokuma, G. A. Voth, P. Salvador, J. J. Dannenberg, V. G. Zakrzewski, S. Dapprich, A. D. Daniels, M. C. Strain, O. Farkas, D. K. Malick, A. D. Rabuck, K. Raghavachari, J. B. Foresman, J. V. Ortiz, Q. Cui, A. G. Baboul, S. Clifford, J. Cioslowski, B. B. Stefanov, G. Liu, A. Liashenko, P. Piskorz, I. Komaromi, R. L. Martin, D. J. Fox, T. Keith, M. A. Al-Laham, C. Y. Peng, A. Nanayakkara, M. Challacombe, P. M. W. Gill, B. Johnson, W. Chen, M. W. Wong, C. Gonzalez, J. A. Pople, Gaussian, Inc., Wallingford CT, **2004**.

[39] G. Micera, E. Garribba, *Dalton Trans.* **2009**, 1914–1918.

[40] ORCA, version 2.6.35, F. Neese, University of Bonn (Germany), **2007**.

[41] B. Cashin, D. Cunningham, P. Daly, P. McArdle, M. Munroe, N. N. Chonchubhair, *Inorg. Chem.* **2002**, *41*, 773–782.

[42] S. Bellemin-Laponnaz, K. S. Coleman, J. A. Osborn, *Polyhedron* **1999**, *18*, 2533–2536.

[43] G. M. Lobmaier, H. Trauthwein, G. D. Frey, B. Scharbert, E. Herdtweck, W. A. Herrmann, *J. Organomet. Chem.* **2006**, *691*, 2291–2296.

[44] A. W. Addison, T. N. Rao, J. Reedijk, J. van Rijn, G. C. Verschoor, *J. Chem. Soc. Dalton Trans.* **1984**, 1349–1356.

[45] T. Jakusch, P. Buglyó, A. I. Tomaz, J. Costa, Pessoa, T. Kiss, *Inorg. Chim. Acta* **2002**, *339*, 119–128.
[46] F. Neese, *J. Inorg. Biochem.* **2006**, *100*, 716–726.
[47] P. E. Riley, V. L. Pecoraro, C. J. Carrano, J. A. Bonadies, K. N. Raymond, *Inorg. Chem.* **1986**, *25*, 154–160.
[48] S. Meicheng, W. Lifeng, Z. Zeying, *Acta Chim. Sinica* **1983**, *41*, 985–992.
[49] C. J. Ballhausen, H. B. Gray, *Inorg. Chem.* **1962**, *1*, 111–122.
[50] E. Garribba, G. Micera, A. Panzanelli, D. Sanna, *Inorg. Chem.* **2003**, *42*, 3981–3987.
[51] A. Abragam, M. Horowitz, M. H. L. Price, *Proc. R. Soc. London Ser. A* **1955**, *230*, 169–187.
[52] R. E. Watson, A. J. Freeman, *Phys. Rev.* **1961**, *123*, 2027–2047.
[53] M. L. Munzarová, P. Kubáèek, M. Kaupp, *J. Am. Chem. Soc.* **2000**, *122*, 11900–11913.
[54] R. LoBrutto, B. J. Hamstra, G. J. Colpas, V. L. Pecoraro, W. D. Frasch, *J. Am. Chem. Soc.* **1998**, *120*, 4410–4416.
[55] G. Roelfes, V. Vrajmasu, K. Chen, R. Y. N. Ho, J.-U. Rohde, C. Zondervan, R. M. la Crois, E. P. Schudde, M. Lutz, A. L. Spek, R. Hage, B. L. Feringa, E. Münck, L. Que, Jr., *Inorg. Chem.* **2003**, *42*, 2639–2653.
[56] I. Nagypál, I. Fábián, *Inorg. Chim. Acta* **1982**, *61*, 109–113.
[57] WINEPR SimFonia, version 1.25, Bruker Analytische MesstechnikGmbH, Karlsruhe (Germany), **1996**.
[58] R. G. Parr, W. Yang, *Density-Functional Theory of Atoms and Molecules*, Oxford University Press, Oxford, **1989**.
[59] A. D. Becke, *J. Chem. Phys.* **1993**, *98*, 5648–5652.
[60] C. Lee, W. Yang, R. G. Parr, *Phys. Rev. B* **1988**, *37*, 785–789.
[61] a) J. P. Perdew, K. Burke, M. Ernzerhof, *Phys. Rev. Lett.* **1996**, *77*, 3865–3868; b) J. P. Perdew, K. Burke, M. Ernzerhof, *Phys. Rev. Lett.* **1997**, *78*, 1396–1396.
[62] a) AOMix program, S. I. Gorelsky, University of Ottawa, **2009**, http://www.sg-chem.net; b) S. I. Gorelsky, A. B. P. Lever, *J. Organomet. Chem.* **2001**, *635*, 187–196.

Received: March 17, 2010
Published online: June 8, 2010

Please note: Minor changes have been made to this manuscript since its publication in Chemistry—A European Journal Early View. The Editor.

